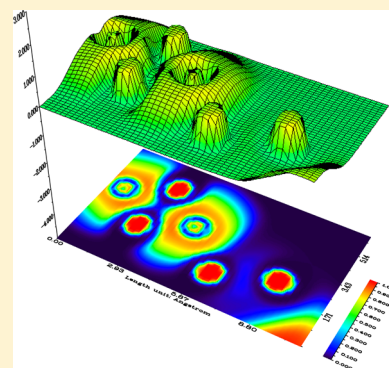


Assemblage of Superalkali Complexes with Ever Low-Ionization Potentials

C. Paduani^{*,†,‡} and Andrew M. Rappe[†]

[†]The Makineni Theoretical Laboratories, Department of Chemistry, University of Pennsylvania, 231 S. 34th Street, Philadelphia, Pennsylvania 19104-6323, United States

ABSTRACT: A simple recipe is proposed for the obtention of new molecules with even lower vertical ionization potential (VIP): to decorate an atom of an electronegative element with superalkali species in number that exceeds its formal valence by one. For instance, density functional theory calculations show that by using the superalkali Li_3O cluster (VIP = 3.83 eV) as building blocks decorating the O atom one obtains VIP = 3.33 eV for the Li_9O_4 cluster, which is lower than the calculated VIP for Cs (3.89 eV) and Li (5.39 eV). This feature is systematic, as confirmed by calculated results on Li–F and Li–S clusters as well. The calculated binding energy per atom of the large-sized species exceeds by far that of LiF (134.7 kcal/mol).



INTRODUCTION

The first ionization potential (IP) is the energy cost to convert an atom into a cation and a free electron. It is a very important quantity, with great relevance to diverse material properties. Elements on the left side of the periodic table have low IPs: ¹Li (5.39), Na (5.14), K (4.34), Rb (4.18), and Cs (3.89 eV). These species play an important role in chemistry, since their excellent reducing ability enables them to form charge-transfer salts when interacting with species with low electron affinity. Gutsev and Boldyrev² showed a recipe for obtaining even smaller IPs following the molecular formula $A_{k+1}C$, where A is an alkali metal atom and C is an electronegative atom with formal valence k . The low IPs of these species is due to the antibonding character of the central atom–ligand interactions. Examples of superalkali are Li_2F , Li_3O , Na_3O , Li_3S , and Li_4N .^{3–5} Among these, Li_2F , Li_3O , Na_3O , and Li_3S indeed have been synthesized,^{6,7} thus confirming the theoretical predictions.

The seeking of alternative candidates to act as potential building blocks to assemble novel low-IP species is timely, and it is important to develop new methods of identifying species with tailored properties. Theoretical predictions have indicated that superatom compounds formed by combining superhalogens (Al_{13}) with superalkalis (K_3O and Na_3O) can exhibit novel chemical and tunable electronic features.⁸ New superalkali–superhalogen compounds $\text{BLi}_6\text{-X}$ ($X = \text{F}$, LiF_2 , BeF_3 , BF_4) have been also theoretically predicted,⁹ where the strong interaction between superalkali and superhalogen X has been found to be ionic in nature. The bond energies of these species are in the range of 151.3–220.6 kcal/mol, which are much larger than the traditional ionic bond energy of 130.1 kcal/mol for LiF. More recently some novel binuclear species have been proposed as superalkalis.^{10,11} A study on a new series of polynuclear cations with various functional groups showed that

the stabilities of these cations are related to the structural characteristics of the central core, and therefore strategies of using acidic functional groups or peroxides for designing novel superalkali cations has been suggested.¹²

In this work is investigated the structure and electronic properties of Li-based supramolecular complexes using density functional theory calculations at the B3LYP/6-311+G(2df) level of theory. The aim is to make an assessment of the feasibility for the obtention of new species with very low ionization potentials using superalkali moieties as building blocks to decorate atoms of the electronegative elements O, F, and S. This procedure follows a simple recipe: CS_{v+1} , where S is a superalkali moiety and C is a central atom of an electronegative element with formal valence v . We choose O, F, and S as candidates for electronegative elements, since there exist both experimental and theoretical results available for comparison. The equilibrium structure, binding energy (per atom), and vertical ionization potential (VIP) are calculated for these species, as well as the dissociation energies along selected channels to observe the thermodynamic stability of these clusters. The results show that the new molecules indeed have appreciably large bond energies and lower VIP than their precursors, which represents a breakthrough to a new level for the ionization potential of highly reactive species.

COMPUTATIONAL METHOD

The calculations based on the density functional theory are performed with the Gaussian-09 package.¹³ The B3LYP exchange-correlation functional is adopted, which combines

Received: June 13, 2016

Revised: July 26, 2016

Published: July 27, 2016

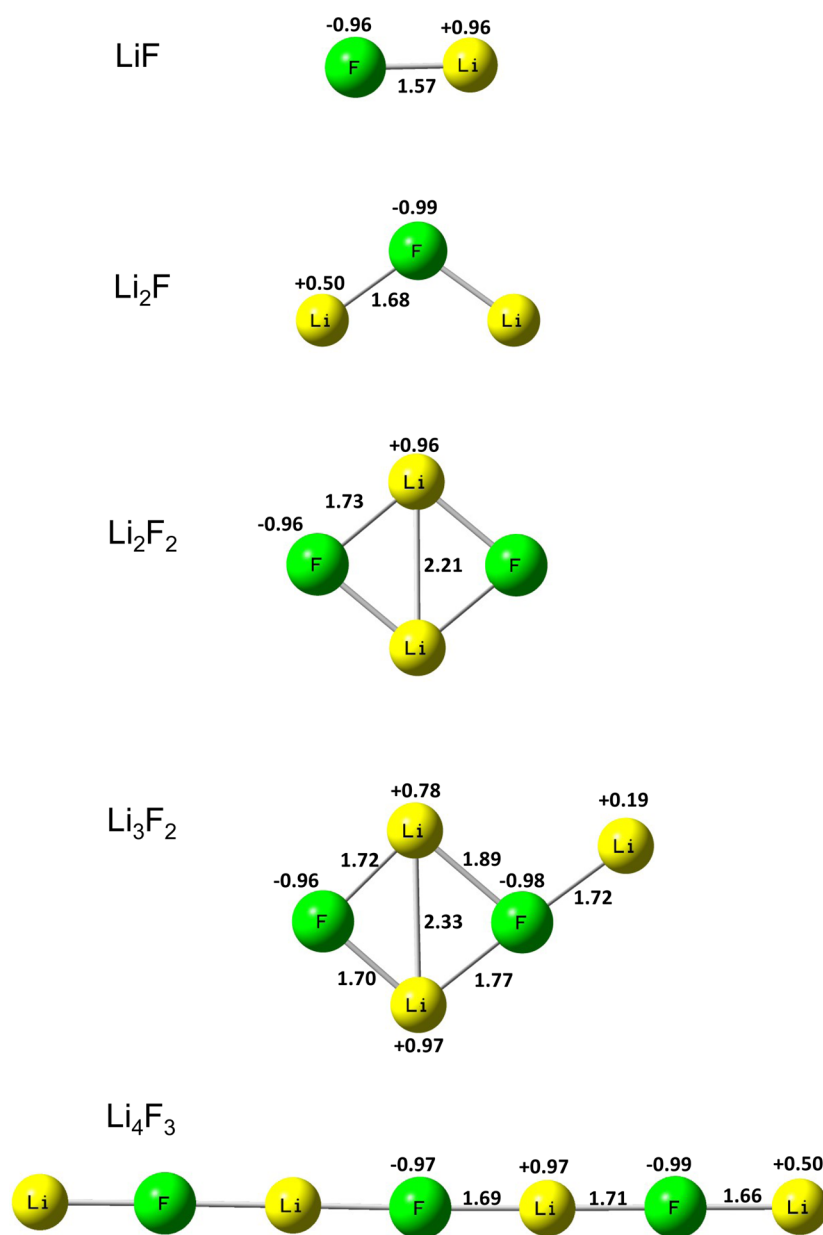


Figure 1. Equilibrium geometries of Li_mF_n clusters; bond lengths (Å) and NAO charges (e) are indicated.

the Becke 3-parameter correlation and the Lee–Yang–Parr hybrid exchange.¹⁴ The 6-311+G(2df) basis set is used throughout. Partial atomic charges were computed by the natural population analysis scheme, which has been proven to be more reliable than other population schemes due to its lower basis set dependency. The equilibrium geometries were obtained by performing multiple optimization runs, each starting from a different geometry of the complex with a careful check for possible isomers, without any constraint in the potential energy surface. Optimized geometries are then characterized by harmonic analysis and by removing any imaginary frequency eventually observed, so that the nature of the stationary points is determined according to the number of negative eigenvalues of the Hessian matrix. Tight convergence thresholds are chosen (i.e., 1×10^{-5} hartree/bohr for the root-mean-squared force), and the residual atomic forces are no larger than 2×10^{-5} hartree/bohr. The VIP is calculated by the difference in the total energies of the neutral cluster and the

cation with the same geometry of the neutral precursor (without relaxation).

RESULTS AND DISCUSSION

Let us begin by describing the equilibrium geometries of the Li–F clusters, shown in Figure 1; significant bond lengths (Å) and natural atomic orbital (NAO) occupancies (e) are indicated. As a general trend among these clusters it is observed that the Li–F bonding is primarily ionic, where Li is an electron donor and F is an acceptor. The Li_2F cluster has a bent shape (C_{2v} symmetry), where the angle $\angle\text{Li–F–Li} = 109.95^\circ$. Compared to LiF, the Li–F bond length in Li_2F increases to 1.68 Å, and the NAO charges on the Li and F atoms are +0.50 and $-0.99 e$, respectively. If another F atom is added to Li_2F the donor–acceptor interactions of the oppositely charged ends of Li_2F_2 thus lead to the joining of the two ends, forming a rhombus cyclic complex (D_{2h} symmetry), as depicted in Figure 1. The Li–F bond length is

1.73 Å, and the angle $\angle\text{F-Li-F} = 100.43^\circ$. Equal and opposite NAO charges are seen on the Li and F atoms (+0.96 and $-0.96 e$, respectively). The equilibrium structure of the Li_3F_2 cluster seen in Figure 1 matches exactly with results of earlier calculations; the present results for the NAO charges and bond lengths also are in very good agreement. Further, by using two Li_2F units as building blocks to decorate a F atom one sees a nearly linear structure (C_{2v} symmetry) for the large Li_4F_3 cluster. Each Li–F unit retains its identity along the chain, where the NAO charges are +0.50, -0.99 , +0.97, -0.97 , +0.97, -0.99 , and +0.50 e , respectively. The terminal Li atoms become weakened donors, with half the charge of the interior Li ions.

In Figure 2 are shown the calculated ground-state geometries of the Li–O clusters. Strong ionic bonding is observed in these clusters. Li_2O is essentially linear. It is noteworthy that the linear geometry has been also deduced from molecular beam experiments.¹⁵ Ab initio calculations with different basis sets also favored a linear $D_{\infty h}$ structure.^{3,16} The Li–O bond length in Li_2O is 1.61 Å, and the NAO charges on the Li and O atoms are +0.95 and $-1.90 e$, respectively. This result, in good agreement with the Li–O distance taken from gas-phase electron diffraction, is 1.60 Å.¹⁷ Li_3O otherwise has trigonal shape (D_{3h} symmetry) reflecting the characteristics of the strong s–p σ -type interactions, where the NAO charges on the Li and O atoms are +0.64 and $-1.92 e$, respectively, and the Li–O bond length is 1.67 Å. With the addition of a second O atom to the Li_3O cluster we see the open-shell cluster Li_3O_2 with D_{3h} . The same NAO charge ($-0.95 e$) is seen on both O atoms; on the Li atoms this is +0.63 e , where the Li–O bond length is 1.81 Å. By using two Li_3O units as building blocks to decorate the O atom is formed the larger Li_6O_3 cluster (D_{3h} symmetry), which has the O atoms aligned and bridged by a triangle of Li atoms, whose NAO charge is +0.92 e on each of them. The two O atoms at the end points have same NAO charge ($-1.81 e$), and the Li–O bond length is 1.72 Å. Next, by decorating the O atom with three Li_3O units we see a nonplanar geometry for the large Li_9O_4 cluster (C_s symmetry) as depicted in Figure 2. The O atoms have approximately same NAO charge, which are bridged to one another through a pair of Li atoms.

Following a similar procedure for the assemblage of the Li–S, we see similar trends in the equilibrium structures throughout the series as illustrated in Figure 3. The bonding mechanism has predominantly strong ionic character and donor–acceptor σ -type interactions in these clusters. Moreover, in addition to the size effect, since sulfur has lower electronegativity as well as lower ionization energy than oxygen, the bond ionicity decreases, as compared to the Li–O clusters, and then we see in Figure 3 longer Li–S bond lengths and smaller NAO charge on the metal atom. Considering the isoelectronic nature of the species the task of finding stability in similar structures is sensible, and a careful check looking for isomers is needed, which demanded several trial calculations starting with different geometries. Note that the metal–chalcogen bonds are slightly stretched, once the size of the complex increases. The properties of the larger complexes are surprising from an electrostatic perspective: all of them are stable equilibrium species with the same C_s structure, strongly bound by 22–52 eV (relatively to isolated atoms).

The calculated VIP and binding energy per atom E_b are summarized in Table 1. This latter is obtained as $E_b = (E_{\text{cluster}} - \sum_{n=1}^N E_n)/N$. For LiF, VIP and E_b are 11.40 and 5.84 eV,

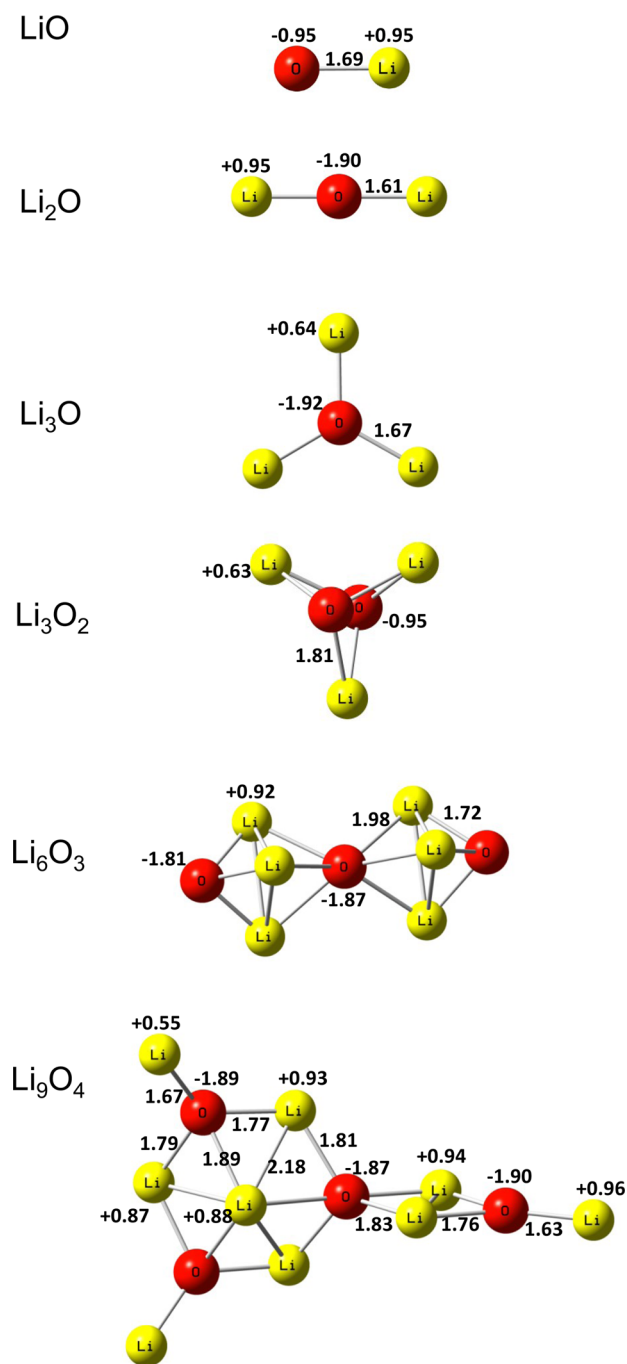


Figure 2. Equilibrium geometries of Li_nO_n clusters.

respectively. For the Li_2F cluster, these are 4.81 and 7.49 eV, respectively. The VIP of Li_2F is thus lower than the VIP of Li (5.61 eV) at the same level of theory. The result of Schleyer³ for the adiabatic ionization potential of Li_2F at the higher level of theory QCISD(T)/6-311+G(2df) is 3.91 eV. When the Li_2F cluster is used for decorating a F atom, the VIP and E_b are 11.80 and 14.46 eV, respectively, for the closed-shell cluster Li_2F_2 . This reveals a strongly bonded complex. For the Li_3F_2 cluster VIP = 4.79 eV, and $E_b = 15.49$ eV. The addition of two Li_2F units decorating the F atom leads to the formation of the larger cluster Li_4F_3 , for which VIP and E_b are 3.48 and 22.92 eV, respectively. This is a remarkable result for VIP, which is significantly lower than that calculated for Cs (3.96 eV) at the same level of theory. The present result for Li_4F_3 thus

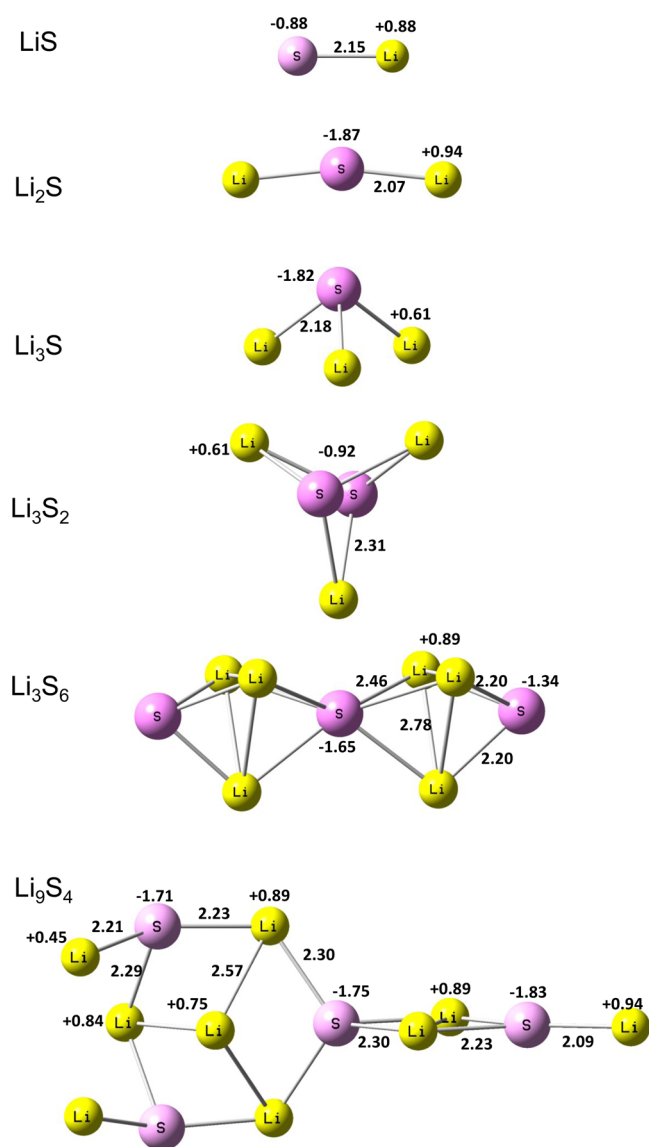
Figure 3. Equilibrium geometries of Li_mS_n clusters.

Table 1. Symmetry, Vertical Ionization Energy, and Binding Energy per Atom

cluster	symmetry	VIP (eV)	E_b^a (eV)
LiF	$C_{\infty v}$	11.40	2.92
Li_2F	C_{2v}	4.81	2.50
Li_2F_2	D_{2h}	11.80	3.62
Li_3F_2	C_s	4.79	3.10
Li_4F_3	C_{2v}	3.48	3.27
Li_2O	C_{2v}	6.67	3.40
Li_3O	D_{3h}	3.86	3.07
Li_3O_2	D_{3h}	3.83	3.64
Li_6O_3	D_{3h}	6.12	3.84
Li_9O_4	C_s	3.33	3.94
Li_2S	C_{2v}	6.63	2.66
Li_3S	C_{3v}	4.52	2.36
Li_3S_2	D_{3h}	3.81	2.86
Li_6S_3	D_{3h}	6.65	3.19
Li_9S_4	C_s	3.78	3.13

^aCalculated at the B3LYP/6-311+G(2df) level.

represents a decrease of $\sim 28\%$ in VIP (compared to Li_2F) and is indeed the lowest value hitherto reported for Li–F clusters. In the same sense of the behavior of the hyperhalogen moieties relative to superhalogens, which represent a step further in increasing the electron affinity, the Li_4F_3 cluster can thus be regarded as a *hyperalkali*, which represents a step further in decreasing IP to a new level. For the Li–O clusters shown in Table 1, we see also a substantial decrease of VIP from Li_2O (6.67 eV) to Li_3O (3.86 eV). A recent calculation reported VIP = 3.85 eV.¹⁸ The experimental result for IP of this cluster is 4.45 eV;¹⁹ this is a superalkali. Proceeding further, by using three Li_3O units to decorate the O atom we see a significant decrease of VIP to the even lower value of 3.33 eV for the large-sized Li_9O_4 cluster. This represents a new level for VIP.

Similarly, when the Li_2S cluster is used as building blocks to decorate the Li atom the calculated VIP decreases from 6.63 to 4.52 eV for the Li_3S cluster. The further addition of a second S atom decreases VIP to 3.81 eV in the open-shell cluster Li_3S_2 . Now, the use of three Li_3S units to decorate a S atom (thus exceeding its formal valence by one) leads to a substantial decrease in VIP to 3.78 eV, revealing again hyperalkali behavior. These results indicate the feasibility for the obtention of new species with VIP even lower than that of the Cs atom. Furthermore, the large-sized clusters possess appreciably larger binding energies. The calculated dissociation energies of these clusters in selected channels are given in Table 2, which gives an estimate of their thermodynamic stabilities relative to

Table 2. Dissociation Energies^a at Selected Channels

channel	eV	kcal/mol
$\text{Li}_2\text{F} \rightarrow \text{LiF} + \text{Li}$	1.65	38.05
$\text{Li}_2\text{F} \rightarrow \text{Li}_2 + \text{F}$	7.49	172.66
$\text{Li}_2\text{F}_2 \rightarrow \text{Li}_2\text{F} + \text{F}$	6.98	160.96
$\text{Li}_2\text{F}_2 \rightarrow \text{Li}_2 + \text{F}_2$	14.46	333.45
$\text{Li}_3\text{F}_2 \rightarrow \text{Li}_2\text{F} + \text{LiF}$	2.16	49.81
$\text{Li}_3\text{F}_2 \rightarrow \text{Li}_2\text{F}_2 + \text{Li}$	1.03	23.75
$\text{Li}_4\text{F}_3 \rightarrow \text{Li}_2\text{F}_2 + \text{Li}_2\text{F}$	0.97	22.37
$\text{Li}_4\text{F}_3 \rightarrow \text{Li}_3\text{F}_2 + \text{LiF}$	1.58	36.55
$\text{Li}_2\text{O} \rightarrow \text{LiO} + \text{Li}$	3.72	85.78
$\text{Li}_2\text{O} \rightarrow \text{Li}_2 + \text{O}$	10.20	235.15
$\text{Li}_3\text{O} \rightarrow \text{Li}_3 + \text{O}$	12.29	283.36
$\text{Li}_3\text{O}_2 \rightarrow \text{Li}_3 + \text{O}_2$	0.67	15.42
$\text{Li}_3\text{O} \rightarrow \text{Li}_2\text{O} + \text{Li}$	2.09	48.20
$\text{Li}_3\text{O}_2 \rightarrow \text{Li}_3\text{O} + \text{O}$	5.90	136.06
$\text{Li}_6\text{O}_3 \rightarrow \text{Li}_3\text{O}_2 + \text{Li}_3\text{O}$	4.11	94.78
$\text{Li}_6\text{O}_3 \rightarrow 2\text{Li}_3\text{O} + \text{O}$	10.01	230.90
$\text{Li}_6\text{O}_3 \rightarrow \text{Li}_2\text{O} + \text{Li}_3\text{O} + \text{LiO}$	5.62	129.70
$\text{Li}_9\text{O}_4 \rightarrow \text{Li}_6\text{O}_3 + \text{Li}_3\text{O}$	4.35	100.31
$\text{Li}_9\text{O}_4 \rightarrow 2\text{Li}_3\text{O}_2 + \text{Li}_3$	14.84	342.33
$\text{Li}_2\text{S} \rightarrow \text{LiS} + \text{Li}$	3.11	71.64
$\text{Li}_2\text{S} \rightarrow \text{Li}_2 + \text{S}$	7.98	184.06
$\text{Li}_3\text{S} \rightarrow \text{Li}_3 + \text{S}$	9.44	217.76
$\text{Li}_3\text{S}_2 \rightarrow \text{Li}_3 + \text{S}_2$	14.31	329.89
$\text{Li}_3\text{S} \rightarrow \text{Li}_2\text{S} + \text{Li}$	1.46	33.67
$\text{Li}_3\text{S}_2 \rightarrow \text{Li}_3\text{S} + \text{S}$	4.86	112.07
$\text{Li}_6\text{S}_3 \rightarrow \text{Li}_3\text{S}_2 + \text{Li}_3\text{S}$	4.92	113.46
$\text{Li}_6\text{S}_3 \rightarrow 2\text{Li}_3\text{S} + \text{S}$	9.78	225.50
$\text{Li}_6\text{S}_3 \rightarrow \text{Li}_2\text{S} + \text{Li}_3\text{S} + \text{LiS}$	6.36	146.78
$\text{Li}_9\text{S}_4 \rightarrow \text{Li}_6\text{S}_3 + \text{Li}_3\text{S}$	2.92	67.34
$\text{Li}_9\text{S}_4 \rightarrow 2\text{Li}_3\text{S}_2 + \text{Li}_3$	12.14	279.86

^aCalculated at the B3LYP/6-311+G(2df) level.

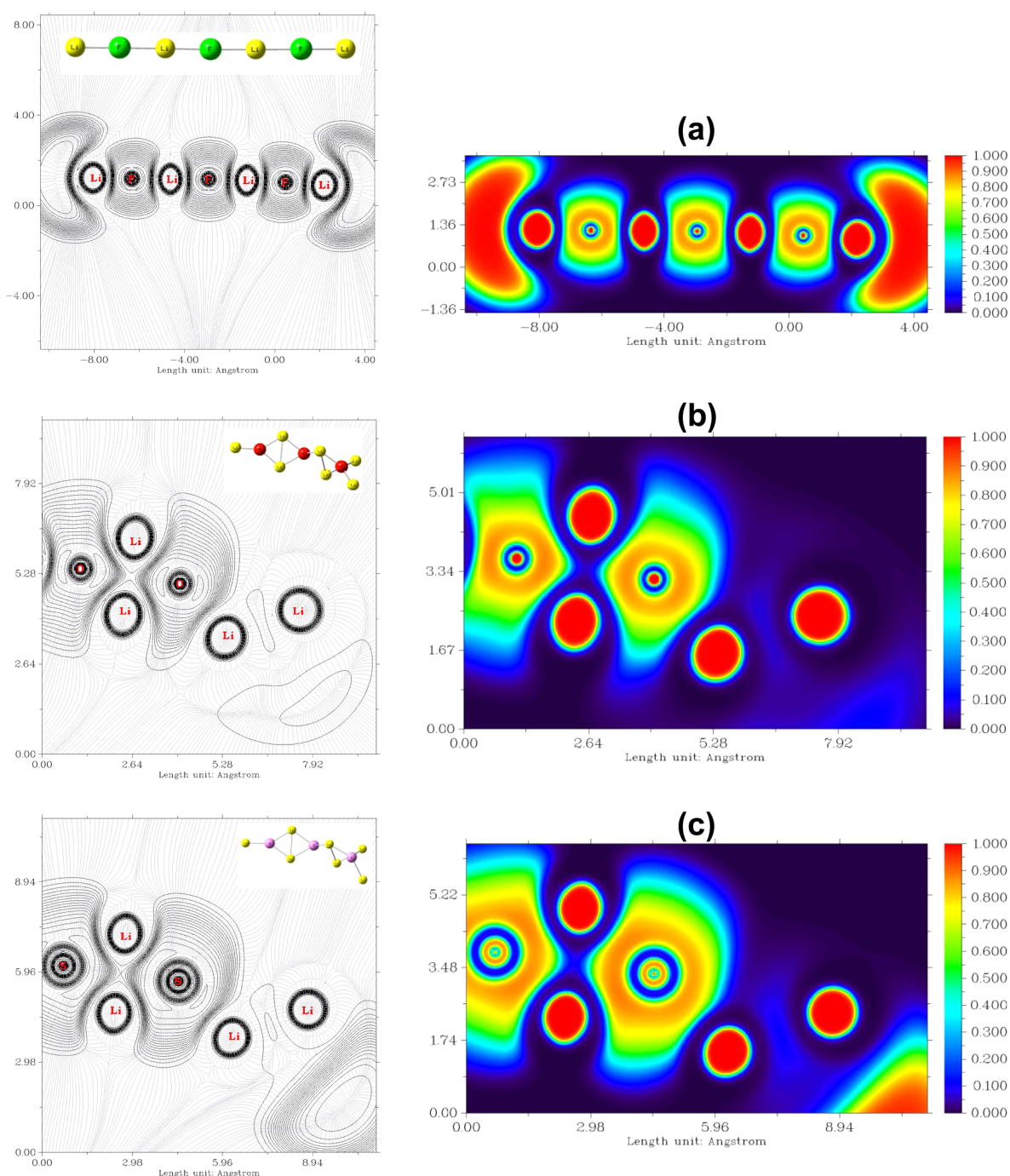


Figure 4. Gradient lines with contour lines (left) and ELF (right) at plane $z = 0$ for the large-sized clusters (a) Li_4F_3 , (b) Li_9O_4 , and (c) Li_9S_4 .

plausible fragments. The results for the smaller clusters compare well with available results of earlier calculations^{18,21} as well as with available experimental results.^{15,16,19,20} The large dissociation energies indicate that these clusters are rather stable. Earlier calculations²¹ give 33.1 for Li_2F , 46.1 kcal/mol for Li_3O , 33.4 kcal/mol for Li_3S , and 40.2 kcal/mol for Na_3O . Experimental results for Li_3S and Na_3O are 50.7 ± 10.0 and 45.4 ± 10.3 kcal/mol,¹⁹ respectively. The lowest fragmentation energy is seen for Li_4F_3 , which shows that this cluster is of the van der Waals type with ionic dipole–dipole interactions. Among the large clusters, the highest stability against dissociation is observed for the Li_9O_4 cluster. Note that the

end Li atoms are holding loosely the extra electron in the neighboring atom, contributing therein to stabilize the cluster.

In Figure 4a–c are displayed plots of the gradient and contour lines (left) as well as of the electron localization function (ELF, right) at the plane $z = 0$ for the larger complexes Li_4F_3 , Li_9O_4 , and Li_9S_4 . In Figure 4a, we can see the antibonding characteristics of the strongly ionic Li–F σ -type sp hybridization, which leads to the linear shape for Li_4F_3 . Despite the less ionic character of the end Li atoms, the delocalized nature of the bonding charge originates equally charged ends and thus provides the driving force to establish the linear arrangement along a chain for this large-sized molecule. As a result of repulsion between valence electrons the

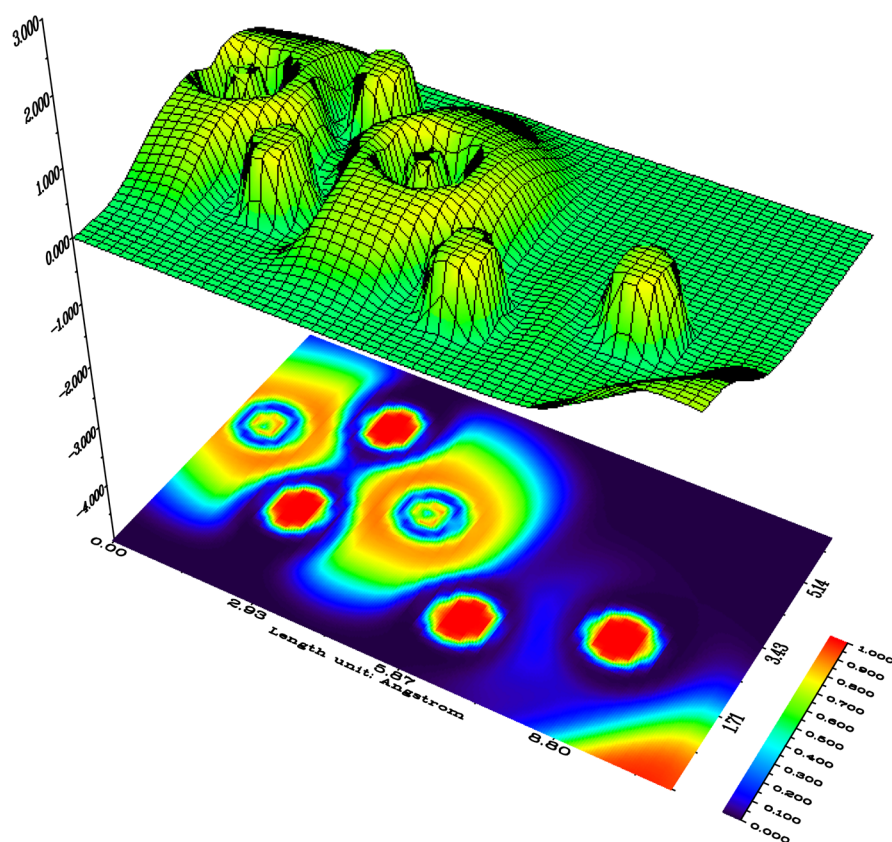


Figure 5. ELF at the plane $z = 0$ for the Li_9S_4 cluster.

bond polarities cancel, and the molecule is nonpolar. In Figure 4b, the interaction between donor–acceptor s – p orbitals dictates the change in the ionicity of the Li – O bonding, affecting the shapes of the diffuse outer lobes of bonding charge, thereby causing the observed bending. Since O is more likely to make twofold coordination than Li , the Li atoms are deployed at end points of the molecule. In the contour plots of Figure 4b,c, note the changes arising from the substitution of S atoms for the O atoms in this plane. The increased delocalization of bonding charge, which provides the conspicuous stability of the large-sized clusters, is also manifestly evident in the color plots (on the right). From a comparison of the plots in Figure 4a–c we see the subtle aspects of the different acceptor character of the electronegative atoms, despite that in these complexes the leading σ -acceptor hybrid is essentially of sp type. The increased electron density on the Li atoms in the Li_9O_4 cluster yields its higher stabilization, whereas the diffuse nature of the outer lobes of the antibonding orbitals leads to the lower stability of the Li_9S_4 complex (Figure 5).

CONCLUSIONS

In summary, we provide theoretical evidence for a new class of supramolecular complexes formed by assembling large-sized Li -based clusters using superalkali clusters as building blocks to decorate the electronegative atoms O , S , and F . First, we observe that the calculated VIPs of the Li_2F (4.81 eV), Li_3O (3.86 eV), and Li_3S (4.52 eV) are smaller than that of the Li atom (5.39 eV). After, when these clusters are used to decorate the corresponding electronegative atom, that is, F , O , and S , respectively, in number that exceeds their formal valence by one, we verify a further decrease in the calculated VIP for the

clusters Li_4F_3 (3.48 eV), Li_9O_4 (3.33 eV), and Li_9S_4 (3.78 eV), which are smaller than that of the Cs atom as well as those of their precursors, and are thus hyperalkali species. These results yield clear evidence to provide a breakthrough in the obtention of new molecules with ever low-ionization energies.

AUTHOR INFORMATION

Corresponding Author

*E-mail: cleudson.paduani@ufsc.br. Phone: +55 (48) 3721 9234. Fax: +55 (48) 3721 9946.

Present Address

‡DF-UFSC, Florianópolis, CEP 88040–900, SC, Brazil.

Notes

The authors declare no competing financial interest.

ACKNOWLEDGMENTS

This research was supported by grants from the Conselho Nacional de Desenvolvimento Científico e Tecnológico (CNPq), Brazil. Computational support from the Centro Nacional de Processamento de Alto Desempenho da Universidade Federal do Ceará (CENAPAD-UFC) and Centro Nacional de Supercomputação da Universidade Federal do Rio Grande do Sul (CESUP, Brazil) are gratefully acknowledged. A.M.R. acknowledges support from the U.S. Department of Energy, Office of Basic Energy Sciences, under Grant No. DE-FG02-07ER46431.

REFERENCES

- (1) Huheey, J. E.; Keiter, E. A.; Keiter, R. L. *Inorganic Chemistry: Principles of Structure and Reactivity*, 4th ed.; HarperCollins: New York, 1993.

- (2) Gutsev, G. L.; Boldyrev, A. I. DVM $X\alpha$ Calculations on the Electronic Structure of "Superalkali" Cations. *Chem. Phys. Lett.* **1982**, *92*, 262–266.
- (3) Schleyer, P. v. R.; Wurthwein, E.-U.; Kaufmann, E.; Clark, T.; et al. Effectively Hypervalent Molecules. 2. Lithium Carbide (CLi_5), Lithium Carbide (CLi_6), and the Related Effectively Hypervalent First Row Molecules, $\text{CLi}_5\text{-nHn}$ and $\text{CLi}_6\text{-nHn}$. *J. Am. Chem. Soc.* **1983**, *105*, 5930–5932.
- (4) Honea, E. C.; Homer, M. L.; Labastie, P.; Whetten, R. L. Localization of an Excess Electron in Sodium Halide Clusters. *Phys. Rev. Lett.* **1989**, *63*, 394–397.
- (5) Honea, E. C.; Homer, M. L.; Whetten, R. L. Electron Binding and Stability of Excess-Electron Alkali Halide Clusters: Localization and Surface States. *Phys. Rev. B: Condens. Matter Mater. Phys.* **1993**, *47*, 7480–7493.
- (6) Neskovic, O. M.; Veljkovic, M. V.; Velickovic, S. R.; Petkovska, L. T.; Peric-Grujic, A. A. Ionization Energies of Hypervalent Li_2F , Li_2Cl and Na_2Cl Molecules Obtained by Surface Ionization Electron Impact Neutralization Mass Spectrometry. *Rapid Commun. Mass Spectrom.* **2003**, *17*, 212–214.
- (7) Yokoyama, K.; Haketa, N.; Tanaka, H.; Furukawa, K.; Kudo, H. Ionization Energies of Hyperlithiated Li_2F Molecule and $\text{Li}_n\text{F}_{n-1}$ ($n = 3, 4$) Clusters. *Chem. Phys. Lett.* **2000**, *330*, 339–346.
- (8) Reber, A. C.; Khanna, S. N.; Castleman, A. W. Superatom Compounds, Clusters, and Assemblies: Ultra Alkali Motifs and Architectures. *J. Am. Chem. Soc.* **2007**, *129*, 10189–10194.
- (9) Li, Y.; Wu, D.; Li, Z. R. Compounds of Superatom Clusters: Preferred Structures and Significant Nonlinear Optical Properties of the $\text{BLi}_6\text{-X}$ ($X = \text{F}, \text{LiF}_2, \text{BeF}_3, \text{BF}_4$) Motifs. *Inorg. Chem.* **2008**, *47*, 9773–9778.
- (10) Tong, J.; Li, Y.; Wu, D.; Li, Z. R.; Huang, X. R. Low ionization potentials of binuclear superalkali B_2Li_{11} . *J. Chem. Phys.* **2009**, *131*, 164307–164311.
- (11) Tong, J.; Li, Y.; Wu, D.; Li, Z. R.; Huang, X. R. Ab Initio Investigation on a New Class of Binuclear Superalkali Cations $\text{M}_2\text{Li}_{2k+1}^+$ ($\text{F}_2\text{Li}^+3; \text{O}_2\text{Li}_5^+, \text{N}_2\text{Li}_7^+$, and C_2Li_9^+). *J. Phys. Chem. A* **2011**, *115*, 2041–2046.
- (12) Tong, J.; Li, Y.; Wu, D.; Wu, Z.-J. Theoretical Study on Polynuclear Superalkali Cations with Various Functional Groups as the Central Core. *Inorg. Chem.* **2012**, *51*, 6081–6088.
- (13) Frisch, M. J.; Trucks, G. W.; Schlegel, H. B.; Scuseria, G. E.; Robb, M. A.; Cheeseman, J. R.; Scalmani, G.; Barone, V.; Mennucci, B.; Petersson, G. A. et al. *Gaussian 09*, Revision E.01; Gaussian, Inc: Wallingford, CT, 2009.
- (14) Becke, A. D. Density-functional thermochemistry. III. The role of exact exchange. *J. Chem. Phys.* **1993**, *98*, 5648–5652.
- (15) Buchler, A.; Stauffer, J. L.; Klemperer, W. J.; et al. Determination of the Geometry of Lithium Oxide, $\text{Li}_2\text{O}(\text{g})$, by Electric Deflection. *J. Chem. Phys.* **1963**, *39*, 2299–2306.
- (16) Mebel, A. M.; Klimenko, N. M.; Charkin, O. P. Structure And Stability of the Lithiated ALi_k And ALi_{k+1}^+ Clusters of the 2nd and 3rd Period Elements by Non-Empirical Calculations with Electronic Correlation Taken into Account. *Zh. Strukt. Khim.* **1988**, *29*, 12–21.
- (17) Tolmachev, S. M.; Zasorin, E. Z.; Rambidi, N. G. Electron Diffraction Study of the Structure of the Vapor-Phase Lithium Oxide Molecule. *J. Struct. Chem.* **1969**, *10*, 449–450.
- (18) Giri, S.; Behera, S.; Jena, P. Superalkalis and Superhalogens as Building Blocks of Supersalts. *J. Phys. Chem. A* **2014**, *118*, 638–645.
- (19) Wu, C. H.; Kudoa, H.; Ihle, H. R. Thermochemical Properties of Gaseous Li_3O and Li_2O_2 . *J. Chem. Phys.* **1979**, *70*, 1815–1820.
- (20) Dao, P. D.; Peterson, K. I.; Castleman, A. W., Jr. The Photoionization of Oxidized Metal Clusters. *J. Chem. Phys.* **1984**, *80*, 563–569.
- (21) Rehm, E.; Boldyrev, A. I.; Schleyer, P. v. R. Ab Initio Study of Superalkalis. First Ionization Potentials and Thermodynamic Stability. *Inorg. Chem.* **1992**, *31*, 4834–4842.